ACS OMEGA

Open Access

This article is licensed under CC-BY-NC-ND 4.0

http://pubs.acs.org/journal/acsodf

Article

Global Proteome Analysis of a Three-Dimensional Human Chondrocyte Cell Culture System Infected with Chikungunya Virus (CHIKV) Reveals Distinct Immune and Inflammatory Signatures

Abdul Hasan,[#] Geetika Sharma,[#] Nilotpal Majumder, Sakshi Chaudhary, Divya Mehta, Raju Vaishya, Sourabh Ghosh,[*] and Sujatha Sunil[*]

Cite This: https://doi.org/10.1021/acsomega.5c02832

Read Online

ACCESS | Metrics & More | Article Recommendations | Supporting Information

ABSTRACT: Chikungunya disease (CHIKD) presents as an acute viral fever with severe joint pain, which may progress into a chronic arthritic condition that can last for months or even years. The cell tropism of chikungunya virus (CHIKV) infection is well studied; however, the mechanisms underlying the pathogenesis of chronicity, especially in the joints, remain poorly understood. Primary chondrocytes were isolated from human joint samples, characterized and grown both as monolayers and as 3D spheroids. These cultures were infected with chikungunya virus (CHIKV) at different multiplicity of infections—(MOIs), and a temporal analysis of infection in these distinct types of culture systems was conducted. Further, the global proteome was obtained from these two kinds of culture systems upon infection, and the proteomes were analyzed in detail to understand the impact of CHIKV on these culture systems. Chondrocytes grown as 3D spheroids were able to sustain CHIKV for extended periods of time, i.e., as long as 168 h, without compromising cellular integrity. Proteomic analysis revealed distinct protein regulation patterns during CHIKV infection, with the changes in 3D spheroids closely resembling those in the natural joint tissue microenvironment. Our study has, for the first time, presented a bird's-eye view of the global proteome changes in human chondrocytes in response to CHIKV infection and further established the usefulness of the 3D chondrocyte culture system in understanding CHIKV infection.

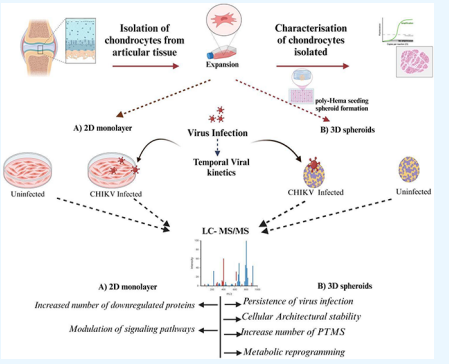

INTRODUCTION

Chikungunya disease (CHIKD) is a debilitating mosquito-borne illness caused by the chikungunya virus (CHIKV), an Alphavirus within the Togaviridae family. The disease typically presents with an acute illness characterized by high fever, maculopapular rash, and incapacitating joint pain. While the fever subsides within days, the joint pain often persists, lasting weeks, months, or even years in chronic cases, severely impacting patients' quality of life.[1] Unlike some mosquito-borne diseases, chikungunya is rarely fatal; however, its economic and social burden is significant, particularly in epidemic regions.[2] The hallmark feature of the disease is the severe joint pain, during which patients experience inflammation of the joints.

CHIKV is transmitted through the bite of an infected *Aedes* mosquito, which deposits the virus in the epidermis. The virus then enters the dermis, spreads across the endothelial barrier, and throughout the body, causing disease symptoms as a result of immune response and inflammation.[3] The virus displays distinct cell and tissue tropism and can efficiently infect endothelial cells, fibroblast cells, muscle cells such as satellite cells and myoblasts, and cells of the joints, including chondrocytes, osteoblasts, and bone marrow mesenchymal stem cells.[4] During the acute phase, the virus infects macrophages and fibroblasts in the synovial joints, leading to an increase in pro-inflammatory cytokines and inducing an immune response primarily involving natural killer cells, B cells, and T cells thus, creating an inflammatory response which induces symptoms of arthritic joint pains.[5] Additionally, some studies have observed that chronic arthritic joint pain in many patients is largely attributed to the persistent presence of the virus within the joint microenvironment.[6] Specific markers related to the immune system have been reported to define disease pathogenicity in different cell types and are known to represent hallmarks of disease progression.[7]

Chondrocytes are resident cell types that reside in the articular cartilage (AC), multiply, and produce an extracellular matrix (ECM) to maintain cartilage homeostasis.[8] These cells establish a microenvironment and are responsible for the turnover of the ECM in their immediate vicinity. In response

Received: April 23, 2025
Revised: July 21, 2025
Accepted: July 28, 2025

Downloaded via 110.225.88.7 on September 11, 2025 at 01:12:38 (UTC).
See https://pubs.acs.org/sharingguidelines for options on how to legitimately share published articles.

ACS Publications

© XXXX The Authors. Published by American Chemical Society

to the inflammatory microenvironment, chondrocyte metabolism changes, which elicits cartilage degeneration and bone erosion.[9] During an arthritogenic virus—infection, chondrocytes are known to be among the cells significantly impacted, playing a crucial role in the progression of viral pathogenesis.[10,11]

Continued efforts toward understanding the acute phase of CHIKD have provided considerable insights into its immunopathology during early infection.[12] Limited *in vivo* studies have shed light on some of the immunological changes that occur during the arthritic phase, but owing to the lack of a defined animal model for CHIKD, the reports lack robust validation.[13] Currently, the C57BL/6 mouse model system has been broadly used to study the *in vivo* pathogenesis of CHIKV. When compared to the disease manifestation in humans, several incongruities have been reported. These mouse models lack major signs of disease that are classically observed in humans, and even if observed, the symptoms disappear within a couple of days of infection.[13] Moreover, it has been noted that a higher dose of viral particles is needed for the disease persistance in mouse models, thereby making these models untenable to study the real disease dynamics.[14] Despite the continued efforts to delineate the pathogenesis of CHIKV, the cellular dynamics of virus infection warrant in-depth investigations. Most importantly, little is known regarding the mechanism of pathogenesis at primary sites of infection, such as macrophages[15] and and joint cells, such as chondrocytes.

In a bid to understand the impact of CHIKV infection on human chondrocytes, we developed a 3D CHIKV infection system using human chondrocytes obtained from human joint samples. Upon characterizing the chondrocytes of the 3D spheroid, we infected the cells with CHIKV, obtained the global proteome upon infection, and analyzed the pathways and perturbed proteins. We identified distinct post-translational modifications in the 2 types of culture systems. We further compared the proteomes of both 2D and 3D cultures, analyzed the perturbations in the pathways caused by CHIKV infection, and observed distinct protein signatures pertaining to immune pathways to be significantly perturbed upon CHIKV infection in 3D chondrocyte spheroids.

MATERIAL AND METHODS

Cell Lines and Virus Strain. The Vero cell line (ATCC) was cultured in Dulbecco's Modified Eagle's Medium (DMEM; Himedia, AL007A) supplemented with 2 mM L-glutamine (Himedia, TCL012), 10% fetal bovine serum (10% FBS), and 1% penicillin−streptomycin (Himedia, A001A) in 5% CO2 at 37 °C. The CHIKV isolate utilized in the study was obtained from an infected patient during a CHIKV outbreak in 2010 (CHIK/DEL/2010/01, Accession No. JF950631.1).[16] The virus was propagated in C6/36 cells (ATCC CRL-1660) in Dulbecco's Modified Eagle's Medium (DMEM; Himedia, AL007A) supplemented with 2 mM L-glutamine (Himedia, TCL012), 10% fetal bovine serum (10% FBS) (GIBCO), and 1% penicillin−streptomycin (Himedia, A001A) in 5% CO_2 incubator at 37 °C for 96 h. The cells were harvested, centrifuged, and the supernatant was collected and stored at −80 °C. The Vero cells were used for virus titter using a plaque assay as previously reported.[17]

Primary Chondrocytes Isolation and Culture. The chondrocytes were isolated from the articular cartilage of human femoral condyles of patients undergoing Total Knee Arthroplasty (TKA) with informed consent and approval from the Institutional Ethics Committee of Apollo Hospital, New Delhi (IAH-BMR-018/10-19). Discarded cartilage samples postsurgery from three patients with the first grade of osteoarthritis were used for this study. The samples were initially washed with PBS mixed with 1% Antibiotic-Antimycotic solution and stored in normal media in the incubator at 37 °C and 5% CO2 for sterility checks. The cartilage blocks were then chopped into 1−2 mm chips and incubated with 0.15% Type-II collagenase solution for 22 h in the incubator. The cartilage chips were strained the next day using a strainer, washed with media twice, and centrifuged at 1500 rpm for 5 min. The pellets obtained were dissolved in media and plated in a cell culture flask for expansion in DMEM supplemented with 1% Antibiotic-Antimycotic, 1 mM sodium pyruvate, 10% FBS, 0.29 g/mL L-glutamine and 100 mM HEPES, and 5 ng/mL Fibroblast Growth Factor-2 (FGF-2).[18]

Characterization of Isolated Chondrocytes. *Histology.* The biopsy sections from the cartilage samples were fixed with 4% formaldehyde, followed by dehydration in graded alcohol concentrations. The tissues were further sectioned into 5-μm-thick fine sections and stained with hematoxylin−eosin (H&E) and Safranin-O, respectively.[19,20]

3-Dimensional (3D) Spheroid Preparation. Chondrocytes were seeded in a 96-well, U-shaped bottom plate with a cell density of 20,000 per well. The plate had been precoated with 2% weight-per-volume poly-HEMA (poly-2-hydroxyethyl methacrylate)[21,22] to prevent cell attachment to the plate surface and facilitate the creation of spheroids. The proliferation medium was used for cell incubation for a duration of 5−7 days, after which well-defined spheroids were obtained.

Chikungunya Virus Infection in Chondrocytes. Isolated chondrocytes from articular joint tissue (passages 2−3) were kept in proliferation media, which consisted of DMEM supplemented with 1% penicillin-streptomycin, 1 mM sodium pyruvate, 10% FBS, and 5 ng/mL FGF2. Chondrocytes grown in a 2D monolayer were infected with CHIKV at a multiplicity of infection (MOI) of 0.1 and 1, whereas the 3D spheroids were infected at MOIs of 0.1, 1, and 10. Chondrocytes infected with an MOI of 1 in 2D monolayer and 3D spheroids were utilized for a global proteomic study.

Proteomic Samples Preparation. Mass spectrometric analysis was performed to evaluate the proteome changes in chondrocytes during CHIKV infection. Chondrocytes were seeded in *T*-75 flasks at a density of 2 million cells per flask and were allowed to grow in 5% CO_2 incubator at 37 °C until 80% confluency. The cells grown in both 2D monolayers and 3D spheroids were infected with the virus for 24 h and kept at 5% CO_2 incubator maintained at 37 °C. After incubation, cells grown in the 2D monolayer were scraped with a sterile cell culture-grade scraper and collected in tubes, while spheroids were collected from 96-well plates. The collected samples were centrifuged and then washed with ice-cold 1X PBS at 4 °C, 200*g*. Following that, the cells were lysed for 15 min on ice using 3 mL of RIPA lysis buffer. After lysis, samples were centrifuged at 10,000*g* for 20 min at 4 °C. The supernatants were collected, and protein concentration was estimated using a BCA protein estimation assay kit (Thermo Fisher Scientific, 23227). Each sample containing 25 μg of protein was digested using trypsin (1:50 trypsin/lysate ratio), further reduced with 5 mM TCEP, and then alkylated with 50 mM iodoacetamide for about 16 h at 37 °C. A silica cartridge C18 was used, and salts

https://doi.org/10.1021/acsomega.5c02832
ACS Omega XXXX, XXX, XXX−XXX

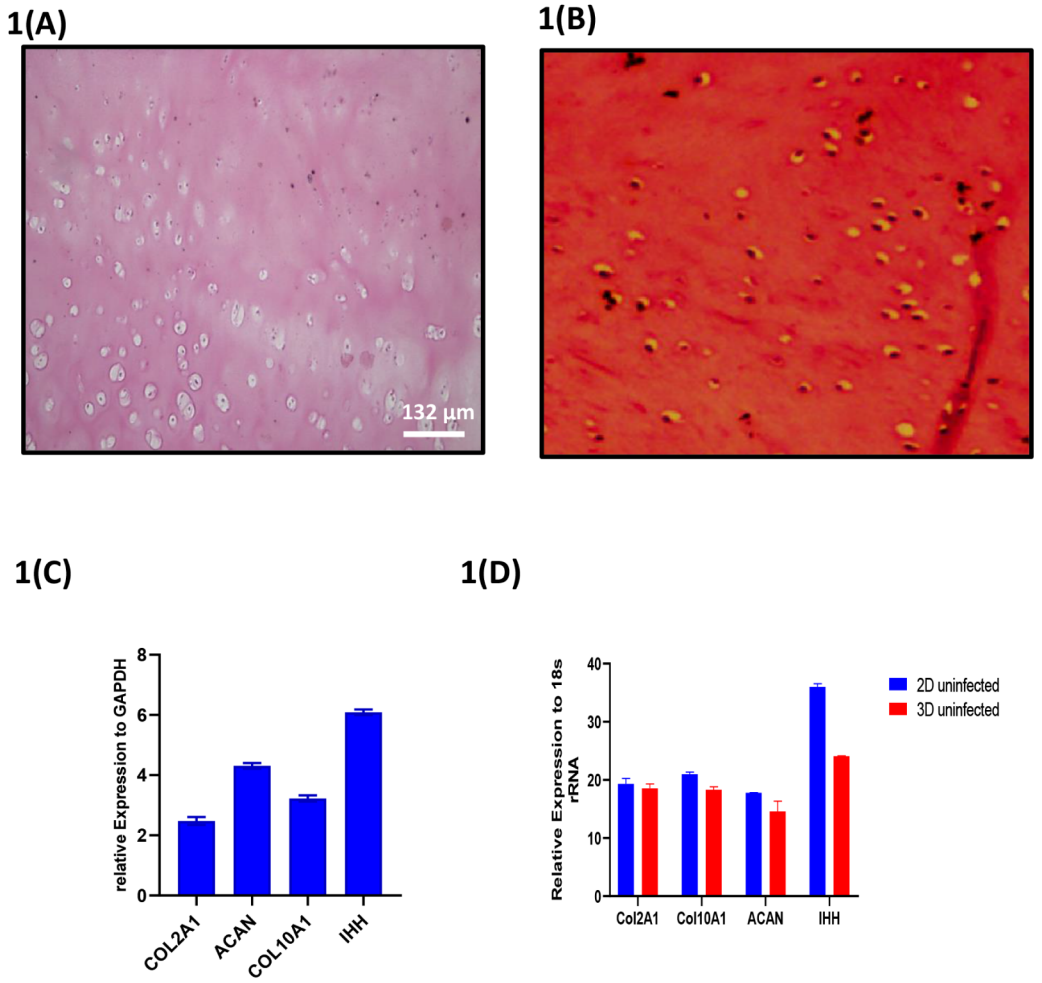

Figure 1. Histology of articular joint tissue and characterization of isolated chondrocytes cultured in vitro: (A) H&E staining of cartilage biopsy tissue from which the chondrocytes are isolated. (B) Safranin-O staining of the cartilage biopsy tissue from which the chondrocytes are isolated showing dense staining of the GAGs. (C) Gene expression analysis of the chondrocytes immediately after isolation relative to the internal control GAPDH. (D) Gene expression analysis of the chondrocytes (uninfected) after the formation of 3D spheroids and 2D monolayers relative to the internal control 18S rRNA. Each experiment was performed in three replicates, and the error bars represent mean ± SD.

were removed and dried with a speed vac (Thermo Fisher Scientific Inc.). Buffer A, with a composition of 1% formic acid and 5% acetonitrile, was used to resuspend the dry pellet.

Mass Spectrometry and Proteomic Change Analysis. NanoLC1200 coupled with a Thermo QE Plus instrument was used for experiments (Thermo Fisher Scientific Inc.). A C18 column measuring 50 cm in length and 3.0 μm in particle size, Easy-spray, was loaded with 1 μg of sample (Thermo Fisher Scientific Inc.). Elution of peptides was performed using a gradient buffer B of 0−40% consisting of acetonitrile (80%, formic acid 0.1%) at a flow rate of 300 nL/min, followed by injection for MS analysis. The LC gradients were run for 100 min. MS1 spectra were obtained in the Orbitrap at a 70K resolution.[23] All charge states for one set of precursors were excluded via dynamic exclusion for 10 s. For acquisition, a linear ion trap was utilized to acquire MS2 spectra at a resolution of 17,500. Samples were processed and analyzed with Proteome Discoverer V2.4 against the Uniport reference database. For Sequest and Amanda's searches, the precursor and fragment mass tolerances were set at 10 ppm and 0.02 Da, respectively.[22,24] The protease used to generate peptides, i.e., enzyme specificity, was set for trypsin/P (cleavage at the C-terminus of "lysine or arginine" unless followed by proline), along with a maximum missed cleavage value of 2. For the database search, carbamidomethylation on cysteine was set as a fixed modification, and methionine oxidation was considered a variable modification. Both the protein false discovery rate and peptide spectrum match were set to 0.01.

Bioinformatics and Statistical Analysis. Protein samples from three biological replicates, each consisting of a CHIKV-infected sample and a time-matched noninfected mock sample, were imported to obtain log2 values. Fold changes were determined for each infected sample compared with their mock samples. The fold changes were analyzed for significance using both Student's *t*-test with two tails and Z-score analysis. All fold changes not deemed significant by the *t*-test were examined by Z-score analysis, expressing each value as its number of standard deviations away from the population mean. For increased stringency, a fold-change cutoff of 1.25-fold dysregulation (≥ 1.25-fold if upregulated or ≤0.80-fold if downregulated) was also applied to proteins deemed significantly dysregulated. Fold changes and *p*-values were imported into the PATHfindR script and KOBAS for additional bioinformatics and pathway analyses. For post-translational modifications (PTM) analysis, MusiteDeep , a deep learning framework for PTM predictions, was down-

https://doi.org/10.1021/acsomega.5c02832
ACS Omega XXXX, XXX, XXX−XXX

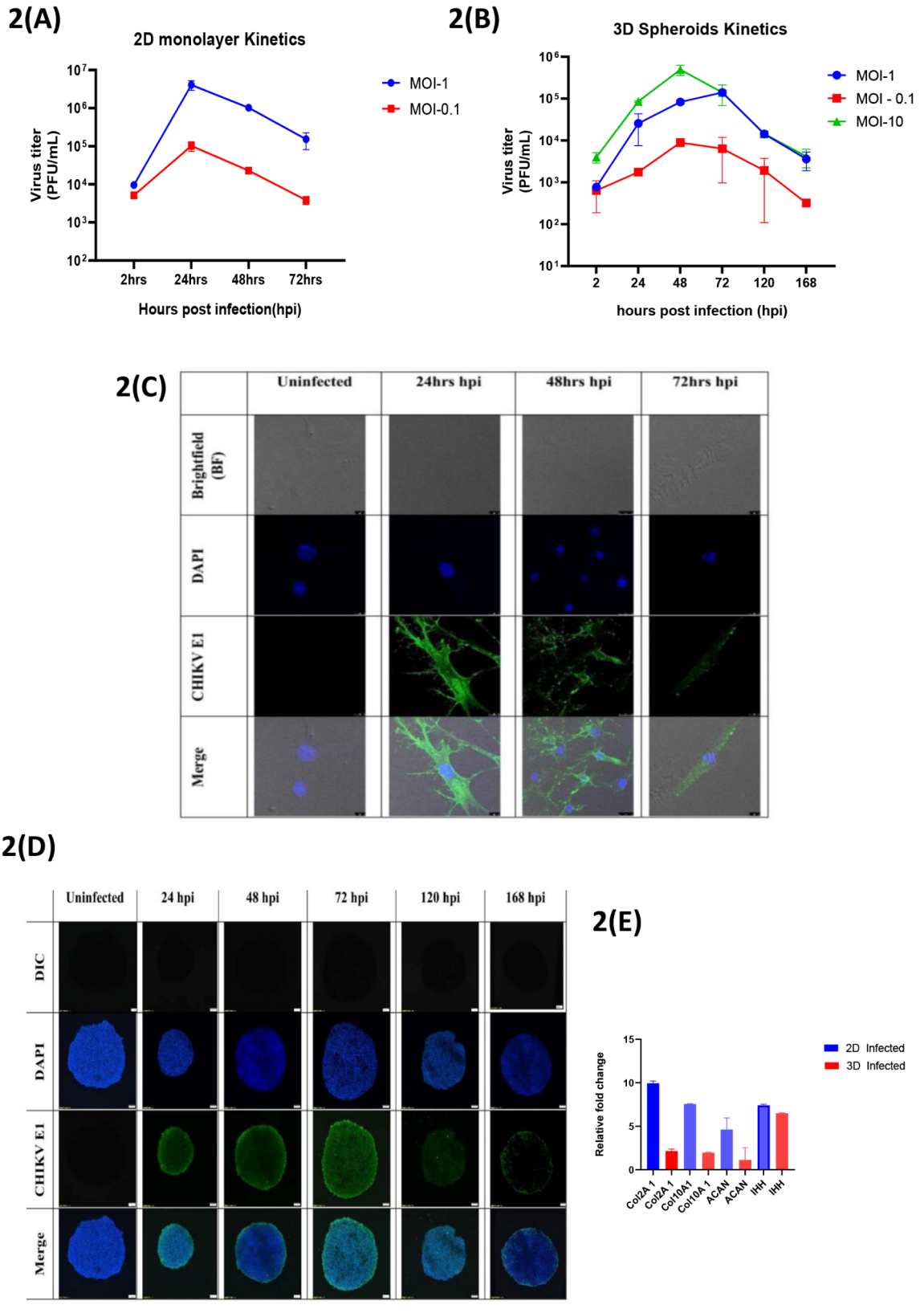

Figure 2. Viral replication profile in chondrocytes cultured in 2D monolayer and 3D spheroid. (A) Plaque assay depicting viral replication kinetics at MOI 0.1 and 1 in chondrocyte monolayers. (B) Plaque assay depicting viral replication kinetics at MOI 0.1, 1, and 10 in 3D spheroid cell models of chondrocytes. Plaque assay data are represented as PFU/mL obtained from three biological replicates, and the error bars represent mean ± SD. (C) Confocal imaging in 2D monolayer for 24, 48,72 hpi. (D) Confocal imaging for 3D spheroidal form for 24, 48, 72, 120, and 168 hpi. The green color represents Alexa 488, an anti-CHIKV envelope protein, and the blue represents DAPI, nucleus. (E) Expression of ECM marker genes in 2D monolayer and 3D spheroidal conditions upon viral infection relative to the internal control 18S rRNA. Each experiment was carried out in three replicates, and mean ± SD is denoted by the error bars.

https://doi.org/10.1021/acsomega.5c02832
ACS Omega XXXX, XXX, XXX−XXX

loaded from its GitHub page. Significant proteins from both 2D monolayer and 3D spheroid conditions were taken further for analysis.

Immunofluorescence Assay for Chondrocytes in 2D Monolayer. Chondrocytes in a 2D monolayer were grown in a 6-well plate at a density of 0.8 million cells per well, containing a sterile glass coverslips seeded 1 day before the assay, i.e., 18 h to allow cell adherence. Cells in the monolayer were infected with CHIKV (MOI 1) for 2 h in serum-free DMEM and its supplements. After 2 h of incubation, 2% DMEM media was added and maintained for up to 72 h post-infection (hpi). The virus-infected cells were collected every 24 h, and washed three times with 1X PBS, and then fixed in 4% formaldehyde for 2 h; after that, PBS washing was performed three times, and permeabilization was carried out using PBST(PBS + 0.5% Triton X-100) for 30 minutes. Again , 1X PBS washing was performed three times, and blocking was done in 2% BSA (PBS + 0.1% Triton X-100) for 1h. The cells were probed with in-house raised CHIKV E1 antibodies[25] at a dilution of 1:200 and incubated at room temperature for 2 h in 2% BSA (PBS + 0.1% Triton X-100). After washing the cells with PBS, they were incubated for another 1 h with goat antimouse IgG Alexa 488-conjugated antibody (1:400 dilution) in the dark at room temperature. Further, the nucleus was stained with DAPI (1:1000), and mounting was performed with 20 μL antifade (Invitrogen). The images were captured by using an inverted confocal laser scanning microscope.

Immunofluorescence Assay for Chondrocytes in 3D Spheroids. For 3D spheroids, chondrocyte cells were seeded in a precoated polyhydroxyethyl methacrylate U-bottom 96-well plate with 20 000 cells per well for about 5 days. After 5 days, when the spheroids had attained optimal morphology, they were infected with the virus at an MOI of 1 for 2 h in serum-free DMEM and its supplements. After incubation, 2% DMEM medium was added, and incubation was continued up to 168 hpi. The infected spheroids were collected every 24 h for further processing. The cells were washed with 1X PBS (thrice), fixed in 4% formaldehyde for 2 h, and permeabilized with PBST (PBS + 0.5% Triton X-100) for 30 min. PBS washing was performed at every intermittent step, and the cells were blocked in 2% BSA (PBS + 0.1% Triton X-100) for 1 h. Upon addition of the primary CHIKV E1 antibody (1:200), the cells were kept at room temperature for 2 h in 2% BSA (PBS + 0.1% Triton X-100). After a 1X PBS wash, spheroids were incubated for another 1 h with goat antimouse IgG Alexa 488-conjugated antibody (1:400 dilution) at room temperature in the dark. Further, staining of the nucleus was performed using DAPI (1:1000). The slides were mounted with 20 μl of antifade (Invitrogen). The images were captured by using an inverted confocal laser scanning microscope (Olympus Fluo-view FV3000).

Gene Expression Profiling Using Quantitative PCR. For the initial characterization of chondrocytes, as described previously,[26] RNA was isolated using freshly isolated cells (day 0) via the RNeasy Mini Kit (Qiagen), followed by reverse transcription with a first-strand cDNA synthesis kit (Thermo Fisher Scientific). Quantitative real-time PCR (qPCR) was carried out on a Rotor-Gene Q thermocycler (Qiagen). Total RNA was extracted from uninfected and infected (24 hpi) monolayer and spheroid cultures of chondrocytes using TRIzol reagent (Thermo Fisher Scientific), and qPCR was performed using the Bio-Rad CFX Opus 96 with the QuantiTect SYBR Green PCR Kit (Qiagen) according to the manufacturer's protocol. Primer details for the host genes probed in the study are provided in Table S1. All reactions were performed in triplicates, and relative gene expression was determined using the Delta Ct method for marker genes (upon isolation and in uninfected monolayer and spheroids). The $2^{-\Delta\Delta Ct}$ method was used to evaluate the fold change in expression of the selected significantly regulated host genes from proteomics data. Data are shown as the mean ± standard deviation (SD).

RESULTS

Isolated chondrocytes exhibited morphological characteristics, and the pattern of gene expression was consistent with articular cartilage (AC) joint tissue. H&E staining of the biopsy section demonstrated spherical chondrocyte morphology embedded within the extracellular matrix (Figure 1A). A noteworthy observation was the difference in cellular morphology and size at different regions of the cartilage sample, with flattened cells in the upper layer to loosely arranged small-sized spherical cells in the intermediate layer and enlarged spherical cells with a tendency for cellular aggregation toward the calcified basal layer. However, dense Safranin-O staining was observed in the cartilage specimen (Figure 1B) indicating the presence of surplus sulfated glycosaminoglycans (sGAG). The gene expression analysis of isolated chondrocytes relative to the internal control, GAPDH, depicted higher expression of chondrogenic ECM marker genes COL2A1 (2.47-fold) and ACAN (4.31-fold). Further, an increased expression of the hypertrophic marker COL10A1 and the IHH signaling pathway ligand IHH gene was also observed (3.22-fold and 6.09-fold, respectively) in the chondrocytes (Figure 1C).

Upon the establishment of the chondrocyte culture, we next proceeded to grow the cells as spheroids and evaluated the marker genes in both the monolayers and spheroids before infecting them with CHIKV. Gene expression analysis revealed an exponential increase in the expression profile of the markers upon passaging compared to their expression upon isolation (Figure 1C,D). Comparing monolayers and spheroids revealed a similar expression profile of Col2A1 Col10A1, and ACAN in both conditions. However, the expression of IHH, a marker associated with chondrocyte proliferation, was significantly higher in the 2D monolayer compared to the 3D spheroid culture, suggesting reduced proliferative activity in the spheroids (Figure 1D).

CHIKV Infection in Chondrocytes Cultured in 2D Monolayer and 3D Spheroid Reveals a Distinct Pattern of Virus Replication Kinetics. Chondrocytes cultured as two-dimensional (2D) monolayers and three-dimensional (3D) spheroids were infected with CHIKV at MOIs of 0.1, 1, and 10. Viral titers were quantified using a standard plaque assay at the indicated time points. In the 2D monolayer cultures, CHIKV titers peaked at 24 hpi, reaching 1.024×10^5 PFU/mL at MOI 0.1 and 4.096×10^6 PFU/mL at MOI 1 (Figure 2A). Following this peak, a progressive decline in viral titers was observed. Notably, significant cell death was evident at 72 hpi at both MOIs, as confirmed by cytopathic effects and confocal microscopy (Figure 2A,C).

In contrast, the infection kinetics in 3D spheroid cultures demonstrated delayed and MOI-dependent viral replication. At an MOI of 0.1, viral titers peaked at 48 hpi (8×10^3 PFU/mL), whereas at an MOI of 1, peak titers were observed at 72 hpi (1.408×10^5 PFU/mL). At of 10, a substantially higher viral load was detected, with titers peaking at 48 hpi ($4.928 \times$

https://doi.org/10.1021/acsomega.5c02832
ACS Omega XXXX, XXX, XXX−XXX

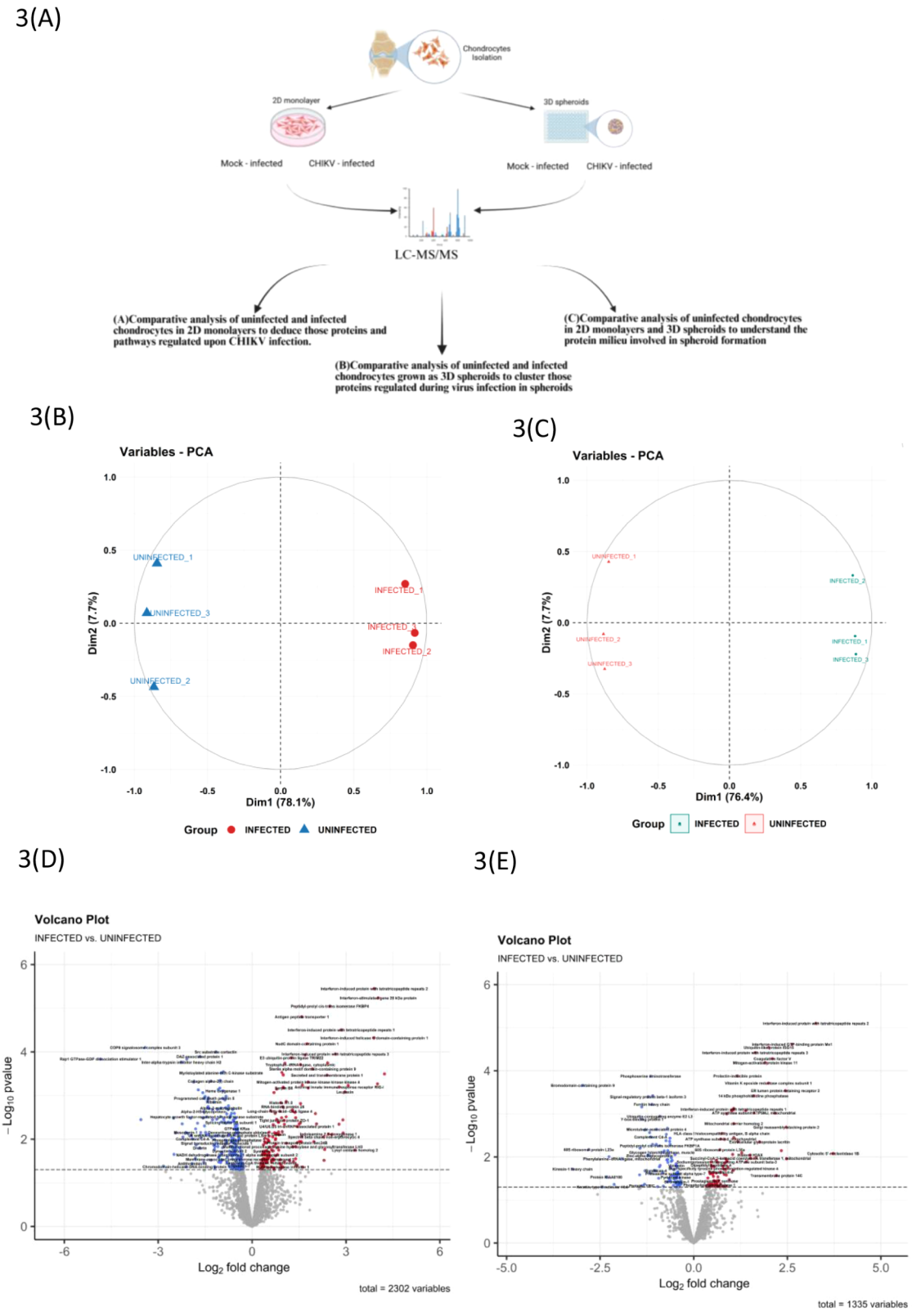

Figure 3. Overview of the study: (A) Flowchart showing the descriptive study undertaken for the proteomics analysis of isolated human chondrocytes during mock or CHIKV infection in 2D monolayer and 3D spheroid cell models. Figure created with BioRender.com (https://BioRender.com/ihgl44g). (B) PCA plot for 2D. (C) PCA plot for 3D. (D) Volcano plot to study upregulated and downregulated proteins in 2D monolayer. (E) Volcano plot to study upregulated and downregulated proteins in 3D spheroid.

10^5 PFU/mL), followed by a sharp decline (Figure 2B). Importantly, the spheroid cultures exhibited sustained viability and structural integrity up to 168 hpi (7 days), in stark contrast to the 2D monolayers, which exhibited pronounced cell death by 72 hpi (Figure 2D).

https://doi.org/10.1021/acsomega.5c02832
ACS Omega XXXX, XXX, XXX−XXX

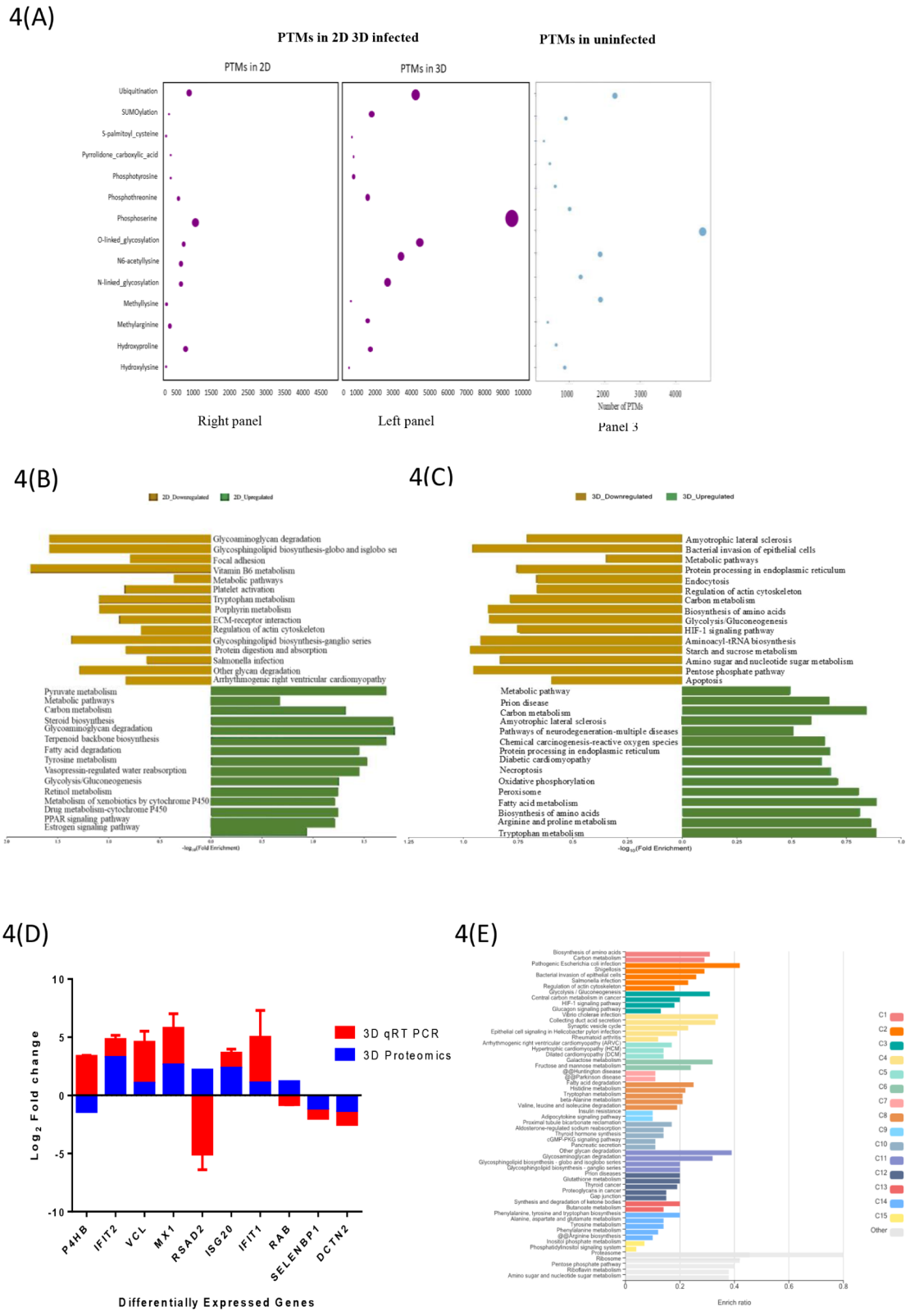

Figure 4. Global proteomic analysis of uninfected vs. infected chondrocytes. (A) Right panel—bubble plot showing the distribution of post-translational modifications (PTMs) in 2D monolayer and 3D spheroid events across various modification types. The *y*-axis lists the different types of PTMs, such as ubiquitination, SUMOylation, and phosphorylation. The *x*-axis represents the number of PTM events recorded for each modification type. The size of each bubble corresponds to the relative abundance or frequency of the respective PTM event. Larger bubbles indicate a higher number of modifications. Panel 3—Bubble plot showing the distribution of post-translational modification (PTM) events in 2D and 3D uninfected datasets across various modification types. The *y*-axis lists the different types of PTMs, such as ubiquitination, SUMOylation, and phosphorylation. The *x*-axis represents the number of PTM events recorded for each modification type. The size of each bubble corresponds to the relative abundance or frequency of the respective PTM event. Larger bubbles indicate a greater number of modifications. (B) Diagrammatic

https://doi.org/10.1021/acsomega.5c02832
ACS Omega XXXX, XXX, XXX−XXX

Figure 4. continued

representation of pathways enriched with up- and downregulated proteins in 2D monolayer cells. (C) Diagrammatic representation of an enriched pathway of up- and downregulated proteins in 3D spheroids. (D) Validation of genes through qRT-PCR. (E) Enrichment analysis of common proteins observed between 2D and 3D uninfected analyses. This process further differentiated the proteins into 15 clusters (C1−C15). C1 represents pathways related to the biosynthesis of amino acids, while C2 represents bacterial invasion of epithelial cell-related pathways. C3 contains pathways of glycolysis. C4 represents rheumatoid arthritis pathways. C5 contains pathways related to cardiomyopathy. C6 represents fructose metabolism pathways. C7 is a class of brain disorder pathways. C8 represents pathways of fatty acid degradation, while C9 represents insulin resistance pathways. C10 represents a group of thyroid-related pathways. C11 contains a pathway related to glycan degradation. C12 contains pathways for glutathione metabolism. C13 is a group of ketone-related pathways. C14 carries pathways from the tyrosine metabolism group. C15 is a group of phosphate metabolism pathways.

To further investigate the impact of CHIKV infection on extracellular matrix (ECM) composition, we assessed the profiling of key ECM-associated genes—COL2A1, COL10A1, ACAN, and IHH—in chondrocytes cultured as either 3D spheroids or 2D monolayers. Quantitative PCR analysis revealed dysregulation of ECM gene expression in 2D monolayers upon CHIKV infection. In contrast, spheroid cultures maintained relative stability in ECM gene expression, with minimal changes observed across most markers. Notably, IHH expression exhibited a 6.4-fold upregulation in spheroids, suggesting a potential role in sustaining cellular signaling or stress response during infection (Figure 2E).

Collectively, these findings suggest that chondrocytes cultured as 3D spheroids are more resilient to CHIKV-induced perturbations, maintaining both molecular and structural integrity over an extended infection period. This contrasts with the 2D monolayer cultures, where early viral replication was accompanied by significant ECM gene dysregulation and cell death, emphasizing the physiological relevance of 3D culture systems for studying CHIKV chronicity-induced pathogenesis.

Global Proteomics Analysis of Chondrocytes 2D Monolayer and 3D Spheroid Reveals Distinct Pattern of Protein Expression with Respect to Cell Architecture and Viral Infection. In order to further characterize the chondrocytes during CHIKV infection, we conducted a comprehensive global proteome analysis of uninfected and CHIKV-infected chondrocytes cultured in a 2D monolayer and 3D spheroids. Based on the replication kinetics findings pertaining to CHIKV infection in the 2D monolayer culture and 3D spheroid, we infected the monolayers and 3D spheroids with CHIKV at an MOI of 1. At 24 hpi, we harvested the cells and performed a global proteome analysis of the infected cells. A detailed work plan for the study is presented in Figure 3A. Principal component analysis (PCA) of the datasets from three biological replicates for uninfected and infected samples revealed distinct clustering of samples based on their infection status in both the 2D monolayer (Figure 3B) and 3D spheroids (Figure 3C). Furthermore, differential expression analysis of the infected and uninfected datasets categorized the proteins based on their regulation, as depicted in the volcano plots (Figure 3D,E).

The data sets were further analyzed to evaluate the impact of CHIKV infection on post-translational modifications (PTMs). A total of 1800 PTM events were observed in the case of chondrocytes grown as 2D monolayers, whereas a significantly larger number of PTMs, i.e., 10,000, were observed in 3D infected chondrocyte spheroids (Figure 4A). The identified PTMs included a diverse range of modifications such as ubiquitination, SUMOylation, phosphorylation, and glycosylation, to name a few (Figure 4). In the 2D environment, PTMs such as phosphorylation and ubiquitination had relatively high frequencies, as indicated by the larger bubble sizes in Figure 4A (left panel). In contrast, 3D spheroids exhibited a broader and more abundant spectrum of PTMs, with a marked increase in phosphorylation and N-linked glycosylation, alongside notable occurrences of methylation and hydroxylation (Figure 4A middle panel). Given the substantial PTM enrichment observed in the 3D infected spheroids, we next profiled PTMs in uninfected chondrocytes under both culture conditions. When the data sets of 2D and 3D uninfected chondrocytes were analyzed, a total of 4762 PTM events were observed (Figure 4A, panel 3). Phosphorylation remained the most frequently detected PTM, followed by SUMOylation and O-linked glycosylation, indicating a baseline regulatory landscape that is further intensified upon viral infection.

To identify the proteins and signaling pathways regulated in response to CHIKV infection, multiple comparative proteomic analyses were performed as follows:

The datasets were further analyzed to identify the proteins and the associated pathways regulated in response to CHIKV infection, and multiple comparative analyses were performed: (1) comparative analysis of uninfected and infected chondrocytes in 2D monolayers to identify infection-specific protein regulation and pathway activation in conventional 2D cultures; (2) comparative analysis of uninfected and infected chondrocytes grown as 3D spheroids to cluster those proteins regulated during virus infection in spheroids; (3) comparative analysis of uninfected chondrocytes in 2D monolayers and 3D spheroids to understand the protein milieu involved in spheroid formation and its potential impact on infection susceptibility and cellular homeostasis. The individual detailed analyses are described below.

(1) Analysis of Proteins and Pathways Regulated upon CHIKV Infection in Chondrocytes Cultured in 2D Monolayer. A bird's-eye view of the cellular changes in CHIKV-infected chondrocyte monolayer culture using proteomic analysis revealed system-wide differences in protein levels. The triplicate data sets of the uninfected and infected samples together yielded 21,486 peptides that translated to 2495 proteins in total. Of these proteins, 59 proteins and 37 proteins were found exclusively in the uninfected and infected data sets, respectively, while 2399 proteins were common to both conditions.

Further, differential expression analysis performed on the proteins common to both groups (n = 2399) identified 147 proteins (Supplementary Sheet 2) to be significantly differentially regulated upon infection with CHIKV, with high protein confidence FDR (p = 0.05; log fold change ± 1). Among the 147 differentially regulated proteins, most were observed to be downregulated (n = 126), while a smaller number (n = 21) were observed to be upregulated. Pathway

https://doi.org/10.1021/acsomega.5c02832
ACS Omega XXXX, XXX, XXX−XXX

analysis of the significantly regulated proteins revealed regulation in cellular pathways such as pyruvate metabolism, carbon metabolism, lysosome pathways, vitamin B6 metabolism, porphyrin metabolism, metabolic pathways, and those modulating the extracellular matrix (Figure 4B).

The most significantly upregulated proteins in the above-mentioned pathways included ME1 (malic enzyme), Isopentenyl-diphosphate Delta-isomerase 1 (IDI1), Methylsterol monooxygenase 1 (MSMO1), Trans-2,3-Enoyl-CoA Reductase (TECR), and Dynein Light Chain LC8-Type 1 (DYNLL1). The downregulated significant proteins impacted in the modulated pathways mentioned above included delta-aminolevulinic acid dehydratase (ALAD), Arylsulfatase B (ARSB), Adenine phosphoribosyltransferase (APRT), Collagen type I alpha 1 chain (COL1A1), Collagen type I alpha 2 chain (COL1A2), and integrin subunit alpha 1 (ITGA1).

(2) Analysis of Proteins Regulated upon CHIKV Infection in Chondrocytes Cultured in 3D Spheroid Cells. Upon analyzing cellular proteome changes accompanying 3D chondrocyte culture, we observed that the triplicate datasets of the uninfected and infected samples together yielded a total of 11,625 peptides that translated to 1383 proteins. Of these 1383 proteins, 14 proteins were found exclusively in the uninfected data sets, and 13 proteins were found in the infected data sets, while 1356 proteins were common to both conditions and were taken for further analysis.

Differential expression analysis of the 1356 common proteins identified a total of 1157 proteins to be significantly regulated with high protein confidence FDR ($p = 0.05$; log fold change ± 1) upon CHIKV infection (Supplementary Sheet 3). Of these 1157 differentially regulated proteins, 508 were observed to be upregulated, and 649 proteins were observed to be downregulated.

Pathway analysis of the differentially regulated proteins identified metabolic pathways, neurodegeneration pathways, amino acid metabolism pathways, and fatty acid metabolism pathways as being significantly upregulated (Figure 4C). Likewise, analysis of the downregulated pathways during infection in 3D chondrocytes revealed that apoptosis pathways, pentose phosphate pathways, glycolysis pathways, endocytosis pathways, and metabolic pathways were the most significantly downregulated.

In-depth scrutiny of the regulated proteins revealed the involvement of important proteins known to participate in significant pathways, such as metabolic, immune, and trafficking, as detailed in Table 1.

In order to validate the global proteomics analysis, we performed targeted qRT-PCR profiling of some of the differentially regulated proteins at their transcript level (Figure 4D). We observed that several factors involved in the structural integrity of cartilage, immune regulation, or inflammatory response, such as vinculin (VCL), collagen (COL), aggrecan (ACAN), proteoglycan (PRG4), interferon-stimulated gene (ISG20), interferon-induced protein with tetratricopeptide repeats (IFIT2), guanosine triphosphate (GTP)-metabolizing protein (MX1), selenium-binding protein (SELENBP1), prolyl 4-hydroxylase enzyme (P4HB), DCTN, RAB, RSAD, IFIT1 aligned with the protein expression patterns observed in the proteomics study.

(3) Comparative Analysis of Chondrocytes in 2D Monolayer Culture and 3D Spheroids. Next, we were interested in investigating the changes that chondrocytes undergo when grown in 2D or 3D cultures to identify the dynamics in cellular architecture when cell types such as chondrocytes, which are dependent on ECM structure and integrity, are cultured in varying *in vitro* conditions. A comparative analysis of chondrocytes in 2D and 3D (uninfected) cultures was performed (Supplementary Sheet 4). Among the unique set of proteins, 2D chondrocyte culture presented 1315 proteins, and 3D culture presented 194 proteins. A total of 978 proteins were identified as being commonly present in both 2D and 3D uninfected

Table 1. Details of the Regulated Proteins and Their Pathways Regulated during CHIKV Infection in Chondrocytes Grown as Spheroids.[a]

Pathways regulated	Protein	−logFC
(A) Metabolic Pathways	Sialin (SLC17A5)	1.012390152
	Inorganic pyrophosphatase (PPA1)	1.031466451
	40S ribosomal protein S14 (RPS14)	1.043621274
	Beta-2-microglobulin (B2M)	1.068943358
	Prolactin-inducible protein (PIP)	1.169838044
	Small nuclear ribonucleoprotein (SNRPE)	1.270836206
	Histone (H2AX)	1.506285209
	Lysozyme C(LYZ)	1.83917355
	Succinyl-CoA:3-ketoacid coenzyme A transferase 1 (OXCT1)	1.515407597
	Kinesin-1 (KIF5B)	−3.237450987
	60S ribosomal protein L23a (RPL23A)	−2.804885462
	PhenylalaninetRNA ligase (FARS2)	−1.923828374
	Protein disulfide-isomerase (P4HB)	−1.387827271
	Dynactin subunit 2 (DCTN2)	−1.15897831
	Glyoxylate reductase/hydroxypyruvate reductase (GRHPR)	−1.15897831
	Phosphoserine aminotransferase (PSAT1)	−1.15086299
	Complement C4-A (C4A)	−1.14817486
	Vinculin (VCL)	1.039596322
(B) Immune Signaling	Interferon-induced protein with tetratricopeptide repeats 1 (IFIT1)[a]	1.062550671
	Tapasin (TAPBP)	1.272876682
	Interferon-induced protein with tetratricopeptide repeats 3 (IFIT3)	1.640194996
	Ubiquitin-like protein (ISG15)[a]	2.001225115
	Radical S-adenosyl methionine domain-containing protein 2 (RSAD2)[a]	2.172164554
	Interferon-stimulated gene 20 kDa protein (ISG20)	2.340080097
	Interferon-induced GTP-binding protein (MX1)	2.628606996
	Interferon-induced protein with tetratricopeptide repeats 2 (IFIT2)[a]	3.262399495
	Early endosome antigen 1 (EEA1)	−1.391412343
	Astrocytic phosphoprotein (PEA15)	−1.467280149
	V-type proton ATPase subunit D (ATP6 V1D)	−1.054107073
	Protein disulfide-isomerase (P4HB)	−1.387827271
(C) Protein Trafficking	Stonin-2 (STON2)	−1.313724964
	Dynactin subunit 2 (DCTN2)	−1.15897831
	Zinc-alpha-2-glycoprotein (AZGP1)	1.179804918
	Sialin (SLC17A5)	1.012390152
	Lipocalin-1 (LCN1)	1.719969267
	Coagulation factor V (F5)	2.100956842

[a]*Represents proteins previously reported in the mouse model (CHIKV).

https://doi.org/10.1021/acsomega.5c02832
ACS Omega XXXX, XXX, XXX−XXX

chondrocytes. Enrichment analysis of these 978 common proteins clustered them into 15 pathways (Figure 4E). The pathway clusters ranged from C1−C15 (Figure 4F) representing pathways primarily related to majorly metabolic pathways,, extracellular matrix, and other biological functions. Analysis of the annotated proteins from the UniProt Knowledgebase (UniProtKB) and the Gene Ontology databases revealed that the majority of the identified proteins were involved in metabolic changes, cytoskeleton organization, and other biological functions. Proteins related to cytoskeleton regulation included Actin beta family members (ACTB, ACTG1, ACTN1, ACTN4), cyclase-associated actin proteins (CAP1, CAPG, CAPN123), cell−cell interaction proteins (CD44, CD47), and collagenase proteins (COL6A1, COL6A2, COL6A3). Overall, we observed that chondrocytes cultured in 2D monolayers and 3D spheroids display unique characteristics, which are altered upon CHIKV infection. The viral infection appears to modulate specific pathways such as arginine, tryptophan, and proline metabolism, as well as Peroxisome and ER pathways, with proteins belonging to these pathways being particularly affected in 3D spheroids, highlighting their distinct biological responses.

DISCUSSION

CHIKD is a complex condition with a limited understanding of the factors that determine disease progression versus resolution. Key factors influencing disease progression include the extent of the host response and the damage caused by the virus to joint tissue. The majority of the current understanding of CHIKV disease biology in joints comes from animal studies; however, small animal models like rats and mice do not mimic the human disease manifestation accurately, which significantly limits the relevance of the information obtained from these studies.[13] In the present study, we utilized the progressive technology of a 3D culture system to study the impact of CHIKV infection in human articular tissue-isolated chondrocyte cells, as this tissue is among the most affected during acute infection and subsequent disease progression. The congruity changes that occur in the tissue are a critical reason for the excruciating pain and impairment experienced by affected individuals. Chondrocytes, along with an extracellular matrix make up the cartilage tissue. Chondrocytes are specialized cells that maintain ECM composition and thus regulate cartilage homeostasis. Collagen, proteoglycans, and water comprise most of the extracellular matrix. These fundamental macromolecules retain water in the cartilage tissue, which also guarantees the cartilage's distinct mechanical characteristics. The structural and operational integrity of cartilage is the responsibility of the ECM; therefore, in order to maintain the normal functioning of cartilage, chondrocytes must generate and arrange the extracellular matrix components.[27] Hence, as an initial quality check to assess the reliability of our chosen cell model, we characterized the chondrocytes we isolated for the study at both the macro- and molecular levels. We observed that the cells displayed characteristics of grade 1 osteoarthritis and near-normal cartilage functioning, with the major portion of the ECM of the articular cartilage evident from dense Safranin-O staining and an upregulated expression of articular cartilage-specific markers COL2A1 and ACAN at the molecular level, indicative of grade 1 OA.[28] While grade 1 OA is characterized by minimal radiographic changes such as doubtful joint space narrowing and possible osteophytic lipping, it is generally considered to represent the earliest and least altered state in the OA continuum, especially when compared to grades 2 and 3, which involve more pronounced structural and metabolic abnormalities.

Targeted gene expression analysis of the marker genes under different conditions of the cells, namely, with and without infection, revealed that 3D spheroids exhibit robust cellular integrity as well as reduced proliferative features. These results were further corroborated through a comparative global proteome analysis. Investigation into the common proteins in the 2D uninfected dataset and the 3D uninfected dataset revealed perturbation of proteins majorly participating in metabolic pathways and those involved in maintaining the cellular cytoskeleton environment. The mechanical properties of the cartilage are maintained by the ECM, which is surrounded and supported by the pericellular matrix, whose development and proliferation depend on COL6A, as observed in our dataset, indicating its role in ECM regulation.[29]

The subsequent key step after characterizing the chondrocytes was to evaluate their capacity to support CHIKV infection under in vitro conditions. Earlier studies have indicated that other alphaviruses, such as Ross River Virus (RRV), could infect chondrocytes effectively. In fact, these reports established that chondrocytes contributed to alphaviral disease pathogenesis by serving as a source of virus replication and soluble factor production.[10] Our replication kinetics demonstrated that CHIKV could successfully infect human chondrocytes, both in a 2D monolayer and when the cells were grown as spheroids. Moreover, it is noteworthy that chondrocytes grown as spheroids were able to sustain CHIKV infection without impacting their cellular integrity and, at the same time, allowed the virus to thrive in the cells for an extended period of time. Most importantly, molecular markers used for the characterization of the chondrocytes during CHIKV infection revealed regulation of several ECM markers, such as Col10A1, IHH, Col2A1, and ACAN, reinforcing the robustness of the cells to sustain virus infection without altering ECM. Previous studies have identified changes in these markers in joint disease conditions where articular cartilage tissue is particularly affected and hypertrophic differentiation of chondrocytes is observed.[30,31] Our data demonstrated that upon viral infection, these markers showed similar regulation, with consistent patterns in both 2D monolayers and 3D spheroids, and more pronounced results observed in the spheroid cultures.

Global proteome analyses of infected chondrocytes in 2D monolayers and 3D spheroids provided interesting information. As this is the first study to evaluate CHIKV infection in spheroids, we compared the results to studies performed in animal models and human subjects. Independent studies have reported the regulation of metabolic pathways[32] in mice infections, including phenylalanine, tryptophan, lysine, arginine, and proline metabolic pathways[33] in the case of DENV infection in humanized mice, ER pathway studies in Avian influenza virus infection in BALB/c mice.[34] These pathways were proven to be significantly regulated in the case of 3D spheroids but were not observed in the 2D monolayer dataset, further emphasizing the relevance of using a 3D culture system to study CHIKV pathogenicity.

Moreover, pathways such as Salmonella infection, Shigellosis, bacterial invasion of epithelial cells, and pathogenic *Escherichia coli* infection, which are typically associated with bacterial pathogens, were found to be enriched in our analysis, thereby highlighting the involvement of host cellular

https://doi.org/10.1021/acsomega.5c02832
ACS Omega XXXX, XXX, XXX−XXX

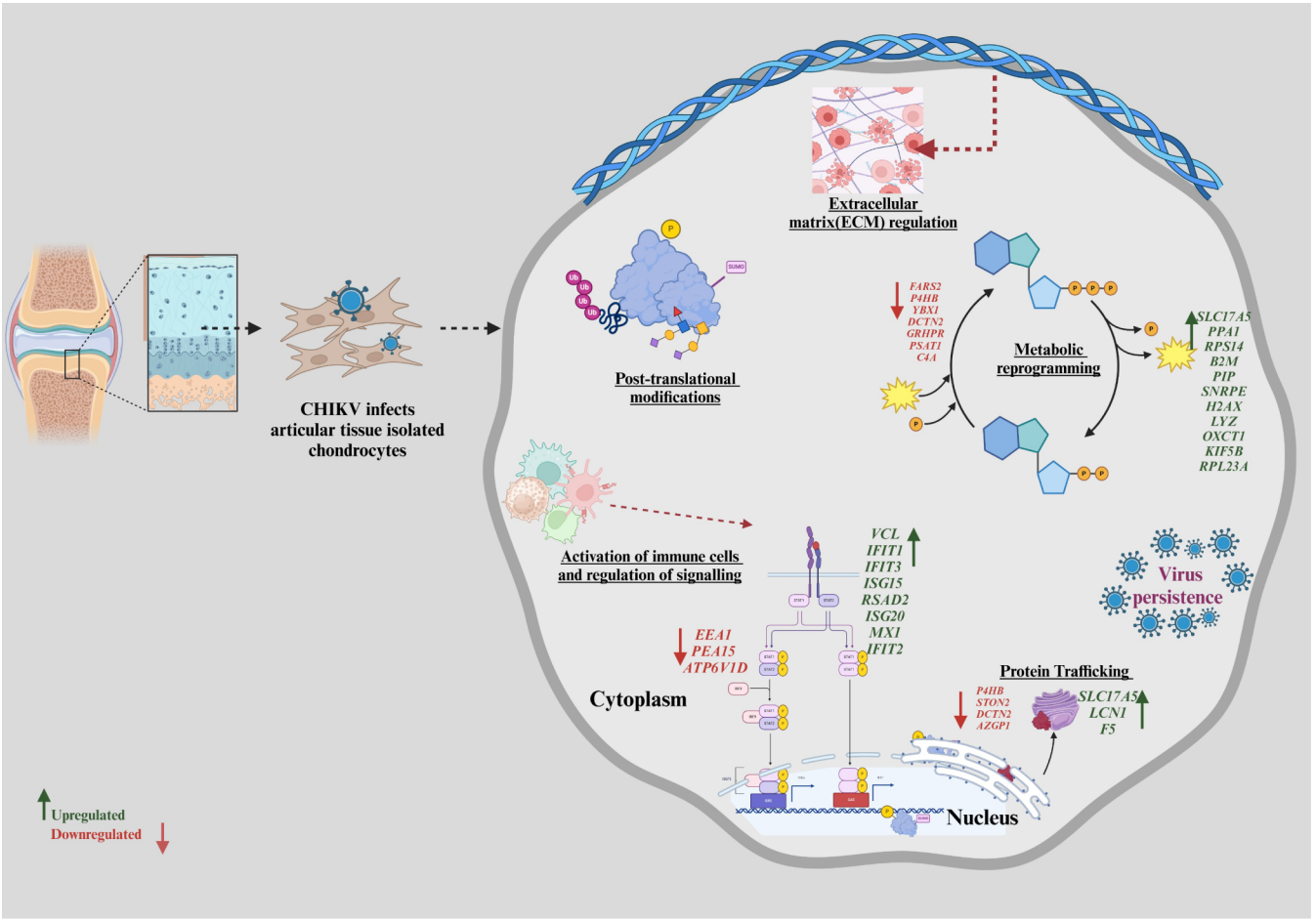

Figure 5. Proposed working model of the changes CHIKV imparts in joint cells based on our 3D global proteomics analysis. CHIKV infection in chondrocytes triggers severe post-translational modifications such as ubiquitination, SUMOylation, phosphoserine-D-linked glycosylation, *N*-6 acetyllysine, and N-linked glycosylation, equipping the cell to combat the virus. Simultaneously, there is activation of immune cells and signaling pathways, which are perturbed by IFIT1, IFIT2, IFIT3, ISG20, ISG15, RSAD2, etc., as they are modulated in the presence of the virus. Immense metabolic reprogramming also takes place via PIP, B2M, OXCT1, RPL23A, and SNPRE. Furthermore, there is modulation of protein trafficking via SLC17A5, LCN1, and F5, which processes biological functions. The most evident outcome of these processes is the persistence of CHIKV, enabling a robust host response that may result in either disease resolution or progression. The chondrocyte spheroid model enables in-depth scrutiny of all the above processes without resorting to animal models. Proteins are denoted in green (upregulated) and red (downregulated) with their respective arrows in the model. Figure created with BioRender.com (https://BioRender.com/rccxpbo).

mechanisms that are critical in the context of cellular integrity also being involved during viral infections, including CHIKV. Many of these bacterial infection pathways converge on cytoskeletal remodeling, a process that is equally essential for viral entry, intracellular trafficking, and egress. The relevance of these enriched pathways extends beyond cytoskeletal regulation. Several canonical immune and inflammatory signaling pathways were also prominently enriched, including cytokine−cytokine receptor interaction, NF-κB signaling, and PI3K-Akt signaling. These pathways are well-documented in CHIKV pathogenesis and contribute to the robust pro-inflammatory cytokine response—especially IL-6, TNF-α, and IL-1β—observed during infection. NF-κB, in particular, plays multiple roles in promoting antiviral defense and contributing to tissue inflammation and joint damage.[35]

Viruses are known to exploit the host machinery to modify their viral proteins for survival, resulting in post-translational modification of host proteins during infection.[36] Among the PTMs observed, phosphorylation and ubiquitination are the most significant, highlighting their roles in modulations of or by the host during infections. For instance, the role of ubiquitination of host proteins is well studied in viruses such as Ebola and Influenza A virus.[37,38] Furthermore, PTMs such as glycosylation have been reported in other flaviviruses such as DENV, ZIKA, and WNV, which aid in virus transmission, entry, and replication.[39,40] It would be worthwhile to study the significance of PTMs during spheroid formation and during CHIKV infection of chondrocyte spheroids at both the systems level and the individual protein level.

Analysis of proteins in the regulated pathways within the chondrocyte 2D monolayer during CHIKV infection revealed the regulation of proteins such as isopentenyl-diphosphate delta-isomerase 1 (IDI1) and RSAD2, which have been extensively studied for their roles in viral pathogenesis. For instance, previous studies have provided insights into the role of IDI1 in modulating cholesterol synthesis to regulate CHIKV replication.[41] The well-defined antiviral role of RSAD2/Viperin in CHIKV is known.[42]

Pathway analysis of the infected spheroids revealed the regulation of metabolic pathways such as arginine and proline metabolism pathways, the peroxisome pathway, and immune-related pathways. CHIKV is known to activate the type I

https://doi.org/10.1021/acsomega.5c02832
ACS Omega XXXX, XXX, XXX−XXX

interferon (IFN) signaling pathway, leading to the production of interferon-stimulated genes (ISGs), which play a crucial role in controlling viral infections.[43] Among these ISGs, IFITs inhibit viral replication through various mechanisms, including suppressing translation initiation[44] binding uncapped or incompletely capped viral RNA, and sequestering viral proteins or RNAs within the cytoplasm of host cells.[45,46] Consistent with these findings, our results showed the upregulation of IFIT2, IFIT3, and ISG15 during CHIKV infection in 3D spheroids. The MxA protein, a cytoplasmic ISG with broad antiviral activity,[47] plays a critical role in controlling viral infections. In neonatal mice, the type I interferon-induced Mx1 has been shown to regulate CHIKV infections[48] which aligns with its upregulation in our 3D spheroid cells.

Together, these findings culminate in a proposed working model that delineates the CHIKV-driven molecular landscape within the joint cells (Figure 5). Our comprehensive 3D global proteomics analysis reveals a multifaceted response of joint cells to CHIKV infection, highlighting widespread post-translational modifications (PTMs) and complex molecular reprogramming. Upon CHIKV infection, chondrocytes undergo extensive PTMs—including ubiquitination, SUMOylation, phosphoserine-linked glycosylation, N6-acetyllysine modification, and N-linked glycosylation—suggesting a coordinated cellular effort to counteract viral invasion. In parallel, immune signaling pathways are markedly perturbed, with upregulation of key antiviral effectors such as IFIT1, IFIT2, IFIT3, ISG15, ISG20, and RSAD2. These interferon-stimulated genes (ISGs) play critical roles in modulating innate immune responses in the presence of the virus. Additionally, our data indicate significant metabolic reprogramming, as evidenced by altered expression of proteins such as PIP, B2M, OXCT1, RPL23A, and SNPRE, which likely reflects an adaptive metabolic shift to support antiviral defense and maintain cellular homeostasis. Moreover, modulation of protein trafficking processes is observed, involving transport-related proteins such as SLC17A5, LCN1, and F5. These changes suggest active remodeling of intracellular trafficking pathways to accommodate the altered proteostasis and signaling demands during infection.

SIGNIFICANCE

This study pioneered the use of 3D spheroid cultures of human chondrocytes to model CHIKV infection, providing a system that closely mimics natural joint tissue. Unlike traditional 2D cell culture systems, the 3D spheroids demonstrated the ability to sustain CHIKV infection for extended periods while maintaining cellular integrity, offering valuable insights into the mechanisms underlying chronic joint pain associated with chikungunya disease. Our findings emphasize the superiority of 3D culture models in replicating in vivo-like conditions and addressing the limitations of existing animal models.

LIMITATIONS

The current study highlights the changes occurring in chondrocytes cultured in both monolayer and spheroidal forms; however, it does not capture the full spectrum of alterations within the cellular environment influenced by interactions with other cell types under natural infection conditions, particularly those involving the immune system. Investigating CHIKV infection in chondrocytes co-cultured with macrophages would offer deeper insights into the host immune response to CHIKV in the joints and also shed light on key inflammatory markers contributing to the arthritic conditions observed in CHIKV-induced arthritis.

CONCLUSION

The present study reinforces the value of 3D culture systems in infection biology, especially in those diseases for which suitable animal models are lacking. The findings from our proteomic analyses highlight various sets of cellular host pathways and proteins that are modulated during disease conditions, laying the groundwork for future investigations into CHIKV-induced arthritis as well as host- pathogen interactions and paving the way for new advancements in therapeutic interventions that would aid in targeting chronic arthritic conditions caused by the virus. Thus, this work advances the understanding of CHIKV-induced arthritis, providing a robust platform for studying disease mechanisms and further testing potential therapies for it.

ASSOCIATED CONTENT

Data Availability Statement

The mass spectrometry proteomics data have been deposited to the ProteomeXchange Consortium via the PRIDE partner repository with the dataset identifier (PXD055872).

Supporting Information

The Supporting Information is available free of charge at https://pubs.acs.org/doi/10.1021/acsomega.5c02832.

Supplementary Table 1 (ST1): list of primes used for real-time PCR. Supplementary Sheet 2: List of *t*-test significant proteins in 2D monolayer; Sheet 3: list of *t*-test significant proteins in 3D spheroids; Sheet 4: list of common proteins in 2D monolayer and 3D spheroids uninfected (PDF)

AUTHOR INFORMATION

Corresponding Authors

Sujatha Sunil − *Vector Borne Diseases Group, International Centre for Genetic Engineering and Biotechnology, New Delhi 110067, India;* orcid.org/0000-0002-1661-482X; Email: sujatha@icgeb.res.in

Sourabh Ghosh − *Department of Textile and Fibre Engineering, Indian Institute of Technology, Delhi 110016, India*; Email: sourabh.ghosh@textile.iitd.ac.in

Authors

Abdul Hasan − *Vector Borne Diseases Group, International Centre for Genetic Engineering and Biotechnology, New Delhi 110067, India;* Present Address: Tulane University, New Orleans, Louisana; orcid.org/0000-0002-0716-7052

Geetika Sharma − *Vector Borne Diseases Group, International Centre for Genetic Engineering and Biotechnology, New Delhi 110067, India*

Nilotpal Majumder − *Department of Textile and Fibre Engineering, Indian Institute of Technology, Delhi 110016, India*

Sakshi Chaudhary − *Vector Borne Diseases Group, International Centre for Genetic Engineering and Biotechnology, New Delhi 110067, India*

Divya Mehta − *Vector Borne Diseases Group, International Centre for Genetic Engineering and Biotechnology, New Delhi 110067, India*

https://doi.org/10.1021/acsomega.5c02832
ACS Omega XXXX, XXX, XXX−XXX

Raju Vaishya − *Indraprastha Apollo Hospital, New Delhi 110076, India*

Complete contact information is available at: https://pubs.acs.org/10.1021/acsomega.5c02832

Author Contributions

#A.H. and G.S. are the co-first authors. S.S. and S.G.: conceptualization; G.S., A.H., and N.M.: methodology; S.C.: bioinformatic analysis; G.S., D.M., and N.M.: validation; S.S.: formal analysis; S.S. and S.G.: resources; S.G. and S.S.: writing—original draft preparation; S.S., G.S., and S.C.: writing—review and editing; S.S. and S.G.: supervision; S.S. and S.G.: funding acquisition. All authors have read and agreed to the published version of the manuscript.

Funding

The work was supported by the Ministry of Ayush (S-14014−12/2019-SCHEME). Institutional Review Board Statement: Scientific and ethical approval to carry out this study was obtained from the Institutional Ethics Committee of Apollo Hospital, New Delhi (IAH-BMR-018/10−19) and the ICGEB Ethics Committee (ICGEB/IEC/2022/44). Consent Statement: Obtained.

Notes

The authors declare no competing financial interest.

■ ACKNOWLEDGMENTS

Mass spectrometric analysis, including sample processing and the run, was conducted at VProteomics Pvt. Ltd., New Delhi, India.

■ REFERENCES

(1) Schwartz, O.; Albert, M. L. Biology and pathogenesis of chikungunya virus. *Nat. Rev. Microbiol.* **2010**, *8* (7), 491−500.
(2) Weaver, S. C.; Forrester, N. L. Chikungunya: Evolutionary history and recent epidemic spread. *Antiviral Res.* **2015**, *120*, 32−39.
(3) Bartholomeeusen, K.; Daniel, M.; LaBeaud, D. A.; Gasque, P.; Peeling, R. W.; Stephenson, K. E.; Ng, L. F.; Ariën, K.K. Chikungunya Fever. *Nat. Rev. Dis. Primers* **2023**, *9* (1), 17.
(4) Hoarau, J. J.; et al. Persistent chronic inflammation and infection by Chikungunya arthritogenic alphavirus in spite of a robust host immune response. *J. Immunol.* **2010**, *184* (10), 5914−5927.
(5) Suhrbier, A. Rheumatic manifestations of chikungunya: Emerging concepts and interventions. *Nat. Rev. Rheumatol.* **2019**, *15* (10), 597−611.
(6) Sourisseau, M.; et al. *Characterization Of Reemerging Chikungunya Virus. PLoS Pathog* **2007**, *3* (6), No. e89.
(7) Archer, C. W.; Francis-West, P. The chondrocyte. *Int. J. Biochem. Cell Biol.* **2003**, *35* (4), 401−404.
(8) Sophia Fox, A. J.; Bedi, A.; Rodeo, S. A. Basic Science Of Articular Cartilage: Structure, Composition, And Function. *Sports Health* **2009**, *1* (6), 461−468.
(9) Lim, E. X.; et al. Chondrocytes Contribute To Alphaviral Disease Pathogenesis As a Source Of Virus Replication And Soluble Factor Production. *Viruses* **2018**, *10* (2), 86.
(10) Lim, E. X. Y.; Webster, J. A.; Rudd, P. A.; Herrero, L. J.; et al. Pathways Activated by Infected and Bystander Chondrocytes in Response to Ross River Virus Infection. *Viruses* **2022**, *15* (1), 136.
(11) Srivastava, P.; Kumar, A.; Hasan, A.; Mehta, D.; Kumar, R.; Sharma, C.; Sunil, S. Disease Resolution In Chikungunya—What Decides The Outcome? *Front Immunol.* **2020**, *11*, 695.
(12) Jain, J.; Narayanan, V.; Kumar, A.; Shrinet, J.; Srivastava, P.; Chaturvedi, S.; Sunil, S. Establishment And Comparison Of Pathogenicity And Related Neurotropism In Two Age Groups Of Immune Competent Mice, C57BL/6J. Using An Indian Isolate Of Chikungunya Virus (CHIKV). *Viruses* **2019**, *11* (6), 578.
(13) Chan, Y. H.; Lum, F. M.; Ng, L. F. P. Limitations of Current in Vivo Mouse Models for the Study of Chikungunya Virus Pathogenesis. *Med. Sci. (Basel)* **2015**, *3* (3), 64−77.
(14) Zhang, Y.; et al. A high-dose inoculum size results in persistent viral infection and arthritis in mice infected with chikungunya virus. *PLoS Neglected Trop. Dis.* **2022**, *16* (1), No. e0010149.
(15) Srivastava, P.; Chaudhary, S.; Malhotra, S.; Varma, B.; Sunil, S.; et al. Transcriptome analysis of human macrophages upon chikungunya virus (CHIKV) infection reveals regulation of distinct signaling and metabolic pathways during the early and late stages of infection. *Heliyon* **2023**, *9* (6), No. e17158.
(16) Shrinet, J.; Jain, S.; Sharma, A.; Singh, S. S.; Mathur, K.; Rana, V.; Bhatnagar, R. K.; Gupta, B.; Gaind, R.; Deb, M.; et al. Genetic characterization of Chikungunya virus from New Delhi reveal emergence of a new molecular signature in Indian isolates. *Virol. J.* **2012**, *9* (1), 100.
(17) Jain, J.; et al. Antiviral Activity Of Ethanolic Extract Of Nilavembu Kudineer Against Dengue And Chikungunya Virus Through In Vitro Evaluation. *J. Ayurveda Integr. Med.* **2020**, *11* (3), 329−335.
(18) Majumder, N.; et al. An Advanced Bioconjugation Strategy For Covalent Tethering Of TGFβ3 With Silk Fibroin Matrices And Its Implications In The Chondrogenesis Profile Of Human BMSCs And Human Chondrocytes: A Paradigm Shift In Cartilage Tissue Engineering. *Adv. Healthcare Mater.* **2024**, *13* (10), 2303513.
(19) Majumder, N.; et al. Covalent Conjugation of Small Molecule Inhibitors and Growth Factors to a Silk Fibroin-Derived Bioink to Develop Phenotypically Stable 3D Bioprinted Cartilage. *ACS Appl. Mater. Interfaces* **2024**, *16* (8), 9925−9943.
(20) Majumder, N.; et al. Immune Response Profiles Induced By Silk-Based Biomaterials: A Journey From 'Immunogenicity'towards 'Immuno-Compatibility. *J. Mater. Chem. B* **2024**, *12* (38), 9508−9523.
(21) Ghosh, S.; et al. Three-Dimensional Culture Of Melanoma Cells Profoundly Affects Gene Expression Profile: A High Density Oligonucleotide Array Study. *J. Cell Physiol* **2005**, *204* (2), 522−531.
(22) Admane, P.; et al. Direct 3D Bioprinted Full-Thickness Skin Constructs Recapitulate Regulatory Signaling Pathways And Physiology Of Human Skin. *Bioprinting* **2019**, *15*, No. e00051.
(23) Dorfer, V.; et al. MS Amanda, a Universal Identification Algorithm Optimized For High Accuracy Tandem Mass Spectra. *J. Proteome Res.* **2014**, *13* (8), 3679−3684.
(24) Das, S.; et al. Enhanced redifferentiation of chondrocytes on microperiodic silk/gelatin scaffolds: Toward tailor-made tissue engineering. *Biomacromolecules* **2013**, *14* (2), 311−321.
(25) Kumar, R.; Mehta, D.; Chaudhary, S.; Nayak, D.; Sunil, S.; et al. Impact of CHIKV Replication on the Global Proteome of Aedes albopictus Cells. *Proteomes* **2022**, *10* (4), 38.
(26) Gentili, C.; Cancedda, R. Cartilage and Bone Extracellular Matrix. *Curr. Pharm. Des* **2009**, *15* (12), 1334−1348.
(27) Chawla, S.; Desando, G.; Gabusi, E.; Sharma, A.; Trucco, D.; Chakraborty, J.; Manferdini, C.; Petretta, M.; Lisignoli, G.; Ghosh, S.; et al. Effect Of silk−gelatin Bioink And TGF-β3 On Mesenchymal Stromal Cells In 3D Bioprinted Chondrogenic Constructs: A Proteomic Study. *J. Chem. Mater. Res.* **2021**, *36* (19), 4051−4067.
(28) Zelenski, N. A.; et al. Type VI Collagen Regulates Pericellular Matrix Properties, Chondrocyte Swelling, and Mechanotransduction in Mouse Articular Cartilage. *Arthritis Rheumatol.* **2015**, *67* (5), 1286−1294.
(29) Neuhold, L. A.; et al. Postnatal expression in hyaline cartilage of constitutively active human collagenase-3 (MMP-13) induces osteoarthritis in mice. *J. Clin. Invest.* **2001**, *107* (1), 35−44.
(30) Nelson, F.; et al. Evidence for altered synthesis of type II collagen in patients with osteoarthritis. *J. Clin. Invest.* **1998**, *102* (12), 2115−2125.
(31) Dhanwani, R.; et al. Characterization of chikungunya virus induced host response in a mouse model of viral myositis. *PLoS One* **2014**, *9* (3), No. e92813.

(32) Cui, L.; Hou, J.; Fang, J.; Lee, Y. H.; Costa, V. V.; Wong, L. H.; Chen, Q.; Ooi, E. E.; Tannenbaum, S. R.; Chen, J.; et al. Serum Metabolomics Investigation of Humanized Mouse Model of Dengue Virus Infection. *J. Virol.* **2017**, *91* (14), 10−1128.
(33) Hrincius, E. R.; et al. Acute Lung Injury Results from Innate Sensing of Viruses by an ER Stress Pathway. *Cell Rep.* **2015**, *11* (10), 1591−1603.
(34) Kumar, R.; et al. Role of Host-Mediated Post-Translational Modifications (PTMs) in RNA Virus Pathogenesis. *Int. J. Mol. Sci.* **2021**, *22* (1), 323.
(35) Selvamani, S. P.; Mishra, R.; Singh, S. K. J. P. O. Chikungunya Virus Exploits Mir-146a To Regulate NF-Kb Pathway In Human Synovial Fibroblasts. *Plos One* **2014**, *9* (8), No. e103624.
(36) Bharaj, P.; Atkins, C.; Luthra, P.; Giraldo, M. I.; Dawes, B. E.; Miorin, L.; Johnson, J. R.; Krogan, N. J.; Basler, C. F.; Freiberg, A. N.; et al. The host E3-ubiquitin ligase TRIM6 ubiquitinates the Ebola virus VP35 protein and promotes virus replication. *J. Virol.* **2017**, *91* (18), 10−1128.
(37) Patil, A.; Anhlan, D.; Ferrando, V.; Mecate-Zambrano, A.; Mellmann, A.; Wixler, V.; Boergeling, Y.; Ludwig, S. Phosphorylation of influenza A virus NS1 at serine 205 mediates its viral polymerase-enhancing function. *J. Virol.* **2021**, *95* (6), No. e02369-20.
(38) Mondotte, J. A.; et al. Essential Role Of Dengue Virus Envelope Protein N Glycosylation At Asparagine-67 During Viral Propagation. *J Virol.* **2007**, *81* (13), 7136−7148.
(39) Carbaugh, D. L.; Baric, R. S.; Lazear, H. M.; Dermody, T. S. Envelope Protein Glycosylation Mediates Zika Virus Pathogenesis. *J. Virol.* **2019**, *93* (12), 10−1128.
(40) Hanna, S. L.; et al. N-linked glycosylation of west nile virus envelope proteins influences particle assembly and infectivity. *J. Virol.* **2005**, *79* (21), 13262−13274.
(41) Thio, C. L.; et al. Differential proteome analysis of chikungunya virus infection on host cells. *PLoS One* **2013**, *8* (4), No. e61444.
(42) Teng, T. S.; et al. Viperin restricts chikungunya virus replication and pathology. *J. Clin. Invest.* **2012**, *122* (12), 4447−4460.
(43) Schoggins, J. W.; et al. A Diverse Range Of Gene Products Are Effectors Of The Type I Interferon Antiviral Response. *Lett* **2011**, *472* (7344), 481−485.
(44) Vladimer, G. I.; Górna, M. W.; Superti-Furga, G. IFITs: Emerging Roles As Key Anti-Viral Proteins. *Front. Immunol.* **2014**, *5*, 94.
(45) Pichlmair, A.; Pichlmair, A.; Lassnig, C.; Baumann, C.L.; Bürckstümmer, T.; Burkard, T.R.; Stefanovic, A.; Bennet, K.; Colinge, J.; Rülicke, T.; et al. IFIT1 Is An Antiviral Protein That Recognizes 5′-Triphosphate RNA. *Nat Immunol.* **2011**, *12* (7), 624−630.
(46) Saikia, P.; Fensterl, V.; Sen, G. C. The inhibitory action of P56 on select functions of E1 mediates interferon's effect on human papillomavirus DNA replication. *J. Virol.* **2010**, *84* (24), 13036−13039.
(47) Haller, O.; Staeheli, P.; Kochs, G. Interferon-induced Mx proteins in antiviral host defense. *Biochimie* **2007**, *89* (6−7), 812−818.
(48) Werneke, S. W.; et al. ISG15 Is Critical In The Control Of Chikungunya Virus Infection Independent Of UbE1l Mediated Conjugation. *PLoS pathogens* **2011**, *7* (10), No. e1002322.


CAS BIOFINDER DISCOVERY PLATFORM™
BRIDGE BIOLOGY AND CHEMISTRY FOR FASTER ANSWERS
Analyze target relationships, compound effects, and disease pathways
Explore the platform
CAS
A division of the American Chemical Society

https://doi.org/10.1021/acsomega.5c02832
ACS Omega XXXX, XXX, XXX−XXX